Journal of Statistics Applications & Probability
An International Journal

http://dx.doi.org/10.18576/jsap/150105

Statistical Inference for Circular and Semi-Circular Generalized Lindley Distributions: Theory and Applications

I. Imliyangba[1], *Mohamed S. Eliwa*[2,3], *Bhanita Das*[1,*], *Partha Jyoti Hazarika*[4], *Mohamed F. Abouelenein*[5], *and Mahmoud El-Morshedy*[6,7]

[1]Department of Statistics, North-Eastern Hill University, Shillong-793022, Meghalaya, India
[2]Department of Statistics and Operations Research, College of Science, Qassim University, Qassim, Saudi Arabia
[3]Department of Statistics and Computer Science, Faculty of Science, Mansoura University, Mansoura 35516, Egypt
[4]Department of Statistics, Dibrugarh University, Dibrugarh, Assam, India
[5]Department of Insurance and Risk Management, College of Business, Imam Mohammad Ibn Saud Islamic University (IMSIU), Riyadh 11432, Saudi Arabia
[6]Department of Mathematics, College of Science and Humanities in Al-Kharj, Prince Sattam bin Abdulaziz University, Al-Kharj 11942, Saudi Arabia
[7]Department of Mathematics, Faculty of Science, Mansoura University, Mansoura 35516, Egypt

Received: 12 Jul. 2025, Revised: 7 Oct. 2025, Accepted: 27 Oct. 2025
Published online: 1 Jan. 2026

Abstract: The incorporation of circular statistics has markedly enhanced the analytical resources accessible to researchers and scientists, especially in contexts where conventional linear probability distributions are inadequate. Numerous real-world phenomena, including directional data, wind directions, temporal patterns, or angular measurements in biology and engineering, demonstrate intrinsic periodicity or circularity, rendering linear models insufficient or deceptive. Circular statistical methods offer a robust foundation for efficiently modeling and analyzing these issues. This article presents a comparative analysis of circular and semi-circular distributions, emphasizing the extension of the established generalized Lindley distribution to these domains. The methods of wrapping and inverse stereographic projection are utilized to convert the generalized Lindley distribution into circular and semi-circular formats, respectively. The resultant circular distribution is designated as the Wrapped Generalized Lindley (WGL) distribution, whereas the semi-circular variant is known as the Semi-Circular Generalized Lindley (SCGL) distribution. The distributions are depicted through linear and circular representations, emphasizing the structural differences and behavioral traits resulting from their geometric transformations. To evaluate their practical applicability, four real-world datasets with semi-circular traits are examined utilizing the proposed distributions. The study examines the efficacy of each model in representing the underlying data patterns and assesses their goodness-of-fit via graphical and statistical comparisons. The results demonstrate that, for the analyzed datasets, the SCGL distribution yields a better match compared to the WGL distribution, indicating that semi-circular modeling presents a more suitable and accurate representation for these data types. This study illustrates the significance of expanding classical distributions into circular and semi-circular domains, equipping researchers with more versatile and precise instruments for the analysis of complex datasets that display periodic or constrained patterns.

Keywords: Circular statistics, Semi-circular distribution, Generalized Lindley distribution, Inverse stereographic projection, Data analysis

1 Introduction

Circular or directed data naturally occur across various scientific and practical disciplines, including biology, geology, geography, meteorology, physics, and medicine. In these fields, researchers frequently confront measures that are intrinsically periodic or directed, rendering conventional linear statistical approaches insufficient. For instance, in

* Corresponding author e-mail: bhanitadas83@gmail.com

© 2026 NSP
Natural Sciences Publishing Cor.

biology, animal movement patterns can be directional; in meteorology, wind directions require analysis as angles; and in medicine, circadian rhythms or the period of disease occurrence may display cyclical activity. The necessity to accurately describe such directions and conduct significant statistical analysis and inference has driven the advancement of circular statistics, a specialist field of statistics tailored for data measured on a circular scale. In a two-dimensional context, directions are depicted as points on the unit circle, with each point corresponding to an angle, typically measured in degrees or radians. This form of data is termed circular data. Conversely, in the context of three-dimensional directions, observations align with points on the unit sphere, symbolizing three-dimensional unit vectors, and are referred to as spherical data. This work concentrates on the two-dimensional scenario, namely circular data. Circular data can be quantified and represented through numerous methods, with the compass and clock being among the most prevalent instruments. Directions on a compass are denoted as angles emanating from a designated reference point (often North) and measured in a clockwise or counterclockwise manner. Illustrations encompass wind directions, ocean current trajectories, avian and animal migratory routes, and the alignment of the Earth's magnetic poles. Time-based circular data can be recorded on a clock over a 24-hour cycle, illustrating occurrences such as patient arrival times at an emergency clinic, seasonal trends in illness prevalence, or monthly and yearly visitor influxes in a city. In compass and clock measurements, it is crucial to establish a zero direction (reference point) and a feeling of rotation (clockwise or anticlockwise) to guarantee that the angles are significant and distinctly defined. In the absence of these specifications, circular data analysis may produce unclear or misleading outcomes. Accurate representation enables researchers to utilize circular statistical approaches, including circular mean, variance, and correlation, which consider the intrinsic periodicity of the data and yield precise insights into directed or cyclical processes.

The eighteenth century signifies the inception of research on directional data. In 1734, Daniel Bernoulli suggested employing the resultant length of normal vectors to assess the homogeneity of unit vectors on the sphere [1]. [2] established a distribution on the circle using a characterization similar to Gauss's characterization of the normal distribution on a line. The application of spherical and circular data was subsequently revitalized by [3], [4], and [5]. [6] expanded the methodologies for Fisher?s distribution and von Mises distribution to address axial data and highlighted the significance of understanding the data type. References [1], [7], [8], and [9] have made substantial contributions through their publications, offering numerous statistical methodologies for the analysis of circular data. Furthermore, [10] delineates the recent remarkable advancements in both theoretical rigor and novel methodologies for applications in directional statistics. Recently, [11] have offered a variety of themes in directional statistics and examined developing trends in directional and multivariate statistics in their book. The concept of encircling a linear distribution around the unit circle is the predominant method for analyzing circular data, resulting in many wrapped circular distributions. [12] initially presented the wrapped distribution, leading to the examination of several wrapped adaptations of prevalent probability distributions on the real line in the literature, such as wrapped normal [8], wrapped Cauchy [9], and wrapped stable distributions [13]. [14] presented a novel circular distribution known as the wrapped Lindley distribution, deriving formulas for the characteristic function, trigonometric moments, skewness coefficients, and kurtosis, along with an application to empirical datasets. In a comprehensive review, [15] cataloged all known wrapped distributions, encompassing 45 distributions for continuous circular data and 10 distributions for discrete circular data. Recently, [16] proposed a more versatile framework for assessing circular datasets by constructing a novel circular distribution that encircles the unit circle, derived from the Chris-Jerry distribution.

The ISP, or bilinear transformation, is a technique for generating both circular and semi-circular distributions from a pre-existing linear model. [17] employed bilinear transformations (Möbius transformations or stereographic projections) to translate points from the unit circle in the complex plane to points on the real line. [18] examined the widely recognized circular model, the circular normal distribution, and produced the associated semi-circular normal distribution. References [19], [20], [21], [22], [23], [24], [25], [26], and [27] have each played a role in the development of stereographic semi-circular distributions using the ISP technique. Recently, [28] introduced a novel two-parameter semi-circular distribution, referred to as the stereographic semi-circular Erlang distribution, developed by the ISP technique. Additionally, a semicircular Maxwell-Boltzmann distribution was introduced by [29], utilizing the ISP approach on the Maxwell-Boltzmann distribution, with a focus on posterior corneal curvature data. The Generalized Lindley (GL) distribution, first described by [30], is a member of the exponential family. The Lindley distribution [31] is clearly a specific instance of the GL distribution when $\alpha = 1$. The GL distribution has garnered much attention in probability literature, enhancing its relevance and applicability. The GL distribution is motivated by its capacity to simulate failure time data characterized by growing, decreasing, unimodal, and bathtub-shaped hazard rates. Furthermore, the majority of studies on GL distribution are confined to random variables possessing an infinite range of potential values. The authors are compelled to implement the concept of circular statistics to the GL distribution by lowering its modulo 2π and π utilizing wrapping and inverse stereographic projection, respectively. The primary aim of this study is to present two novel distributions. A generalized Lindley distribution has been introduced by encircling the density along a unit circle, referred to as the WGL distribution. Conversely, a semi-circular distribution is formulated utilizing the ISP approach, referred to as the SCGL distribution, in which observations are confined to a half-circle, specifically inside the interval $[0, \pi)$. A comparative analysis will be undertaken on the newly proposed distributions,

© 2026 NSP
Natural Sciences Publishing Cor.

namely the WGL and SCGL distributions. It is evident that a dataset containing points within the range of 0 and π will most appropriately conform to a semi-circular model or distribution. The authors aim to apply this theory by fitting two semi-circular real-world datasets to both WGL and SCGL distributions and analyzing the outcomes.

The remainder of the paper is structured as follows: Section 2 delineates the methodology of the wrapping technique and the inverse stereographic projection (ISP) approach, accompanied with the probability density function (PDF) and cumulative distribution function (CDF) of the WGL and SCGL distributions, respectively. Section 3 illustrates the graphical representations (linear and circular) of WGL and SCGL distributions, while Section 4 examines various trigonometric moments and associated features of these distributions. Section 5 applies the WGL distribution to two real-world datasets to demonstrate its applicability, while section 6 examines two real-world datasets to compare the performances of the WGL and SCGL distributions and identify the superior match. Ultimately, the section provides the concluding remarks.

2 The WGL and SCGL Distributions: Mathematical Theory and Visualization

This section discusses the methodologies of the wrapping approach and the ISP method. The techniques are likewise employed to produce WGL and SCGL distributions utilizing the GL distribution. The pdf and cdf of the WGL and SCGL distributions are derived in the subsequent sub-sections.

2.1 The WGL Distribution: Mathematical Theory

Any linear random variable (r.v) X defined on the real line can be transformed into a circular random variable by considering its value modulo 2π. Formally, we define:

$$\theta = X \pmod{2\pi}, \quad \theta \in [0, 2\pi).$$

This operation corresponds to taking the real line and wrapping it around a circle of unit radius. In this mapping, all points on the line that differ by integer multiples of 2π are identified with the same point on the circle. That is, probability mass at $x = \theta, \theta \pm 2\pi, \theta \pm 4\pi, \ldots$ accumulates at the circular position θ. Clearly, this is a many-to-one mapping, and if $g(\theta)$ represents the circular density and $f(x)$ is the density of the linear random variable, the circular density is expressed as

$$g(\theta) = \sum_{m=-\infty}^{\infty} f(\theta + 2\pi m), \quad 0 \leq \theta < 2\pi. \tag{1}$$

Equation (1) forms the basis for constructing both discrete and continuous wrapped distributions. By wrapping a linear distribution around the circle, we can model periodic or directional phenomena that cannot be adequately described by standard linear distributions. The generalized Lindley (GL) distribution, introduced by [30], is defined on the positive real line and has the following pdf:

$$f(x; \lambda, \alpha) = \frac{\lambda^2}{\alpha(\lambda + \alpha^2)}(1 + \alpha x) \exp\left(-\frac{\lambda}{\alpha} x\right), \quad x > 0,\ \lambda > 0,\ \alpha > 0, \tag{2}$$

with the corresponding CDF given by

$$F(x) = 1 - \frac{\alpha(\lambda + \alpha^2) + \lambda \alpha^2 x}{\alpha(\lambda + \alpha^2)} \exp\left(-\frac{\lambda}{\alpha} x\right). \tag{3}$$

Applying the wrapping technique of Equation (1) to the GL distribution, we obtain the PDF of the WGL distribution:

$$\begin{aligned} g(\theta) &= \sum_{m=0}^{\infty} f(\theta + 2\pi m) \\ &= \sum_{m=0}^{\infty} \frac{\lambda^2}{\alpha(\lambda + \alpha^2)} [1 + \alpha(\theta + 2\pi m)] \exp\left(-\frac{\lambda}{\alpha}(\theta + 2\pi m)\right) \\ &= \frac{\lambda^2}{\alpha(\lambda + \alpha^2)} \exp\left(-\frac{\lambda}{\alpha}\theta\right) \left\{ \frac{1 + \alpha\theta}{1 - e^{-2\pi\lambda/\alpha}} + \frac{2\pi\alpha e^{-2\pi\lambda/\alpha}}{(1 - e^{-2\pi\lambda/\alpha})^2} \right\}. \end{aligned} \tag{4}$$

© 2026 NSP
Natural Sciences Publishing Cor.

Similarly, the CDF of the WGL distribution can be expressed as:

$$G(\theta) = \frac{1}{1-e^{-2\pi\lambda/\alpha}}\left\{1-\exp\left(-\frac{\lambda}{\alpha}\theta\right)-\frac{\lambda\alpha^2\theta}{\alpha(\lambda+\alpha^2)}\exp\left(-\frac{\lambda}{\alpha}\theta\right)\right\} + \frac{2\pi\lambda\alpha^2}{\alpha(\lambda+\alpha^2)}\left(1-\exp\left(-\frac{\lambda}{\alpha}\theta\right)\right)\frac{e^{-2\pi\lambda/\alpha}}{(1-e^{-2\pi\lambda/\alpha})^2}. \quad (5)$$

The WGL distribution inherits the flexibility of the generalized Lindley distribution, while simultaneously respecting the periodic nature of circular data. Its PDF can take a variety of shapes depending on the parameters λ and α, including skewed and unimodal forms, which makes it particularly suitable for modeling directional phenomena such as wind directions, animal movement, and cyclic temporal data. Moreover, the wrapping technique ensures that probability mass is accumulated over all possible rotations of the circle, providing a coherent probabilistic framework for circular data analysis. The wrapped transformation highlights the conceptual shift from linear to circular modeling. While the original GL distribution is defined on $[0,\infty)$, the WGL confines the support to the circle $[0,2\pi)$ and naturally accounts for the periodicity of angular measurements. This approach also allows extensions to discrete and continuous distributions, making it a versatile tool for both theoretical derivations and practical applications in circular statistics.

2.2 The SCGL Distribution: Mathematical Theory

Let $f(x)$ and $F(x)$ denote the PDF and CDF of a linear random variable X, respectively. Similarly, let $m(\theta)$ and $M(\theta)$ denote the PDF and CDF of a random point θ on the unit circle. By using a suitable transformation, the circular or semi-circular functions $m(\theta)$ and $M(\theta)$ can be expressed in terms of the linear functions $f(x)$ and $F(x)$. For a positive scaling parameter $v>0$, we have:

$$M(\theta) = F\left\{u+v\,\tan\left(\frac{\theta}{2}\right)\right\} = F\big(x(\theta)\big),$$

$$m(\theta) = v\left\{\frac{1+\tan^2\left(\frac{\theta}{2}\right)}{2}\right\} f\left\{u+v\,\tan\left(\frac{\theta}{2}\right)\right\}.$$

Here, u and v are location and scale parameters, respectively. These equations represent a general inverse stereographic projection (ISP) transformation, which maps a linear variable X onto a semi-circle. By setting $u=0$ and $v=1$, we obtain the **modified ISP**, which simplifies the transformation to:

$$M(\theta) = F\left\{\tan\left(\frac{\theta}{2}\right)\right\},$$

$$m(\theta) = \frac{1}{2}\sec^2\left(\frac{\theta}{2}\right) f\left\{\tan\left(\frac{\theta}{2}\right)\right\}.$$

This modified ISP provides a convenient approach to construct semi-circular distributions from linear distributions, effectively mapping the real line to the semi-circle $[0,\pi)$. Applying this transformation to the GL distribution results in the SCGL. The PDF of the SCGL distribution is obtained as:

$$m(\theta) = \frac{1}{1+\cos\theta}\frac{\lambda^2}{\alpha(\lambda+\alpha^2)}\left\{1+\alpha\tan\left(\frac{\theta}{2}\right)\right\}\exp\left\{-\frac{\lambda}{\alpha}\tan\left(\frac{\theta}{2}\right)\right\}, \quad 0\le\theta<\pi,$$

and the corresponding CDF is given by:

$$M(\theta) = 1-\frac{\alpha(\lambda+\alpha^2)+\lambda\alpha^2\tan\left(\frac{\theta}{2}\right)}{\alpha(\lambda+\alpha^2)}\exp\left\{-\frac{\lambda}{\alpha}\tan\left(\frac{\theta}{2}\right)\right\}.$$

The SCGL distribution is particularly useful for modeling semi-circular data where observations are naturally constrained to a half-circle, such as directional measurements restricted to a single quadrant, partial-day time data, or angular measurements with physical boundaries. The use of the modified ISP ensures that the transformation preserves the probabilistic structure of the original GL distribution while mapping it to the semi-circular domain. The factor $(1+\cos\theta)^{-1}$ in the PDF accounts for the curvature of the semi-circle, ensuring that the total probability integrates to 1. Compared to circular distributions, the SCGL provides a more accurate representation for data confined to a semi-circle, improving the fit for practical applications in meteorology, biology, and engineering.

© 2026 NSP
Natural Sciences Publishing Cor.

3 Graphical Representations of WGL and SCGL Distributions

Continuous distributions are generally characterized by probability density functions (PDFs), depicted as continuous curves. The graphical depiction of a probability density function is essential for illustrating the behavior of a continuous random variable and for evaluating the probabilities linked to various outcomes. The curve's shape indicates significant distributional attributes, including skewness, modality, and tail behavior, while the total area beneath the curve quantifies probability. Graphical representations of the WGL and SCGL distributions are produced to emphasize these characteristics for different parameter combinations of λ and α. These visualizations highlight the impact of parameter alterations on the general form and dispersion of the distributions. Furthermore, both linear and circular depictions of the WGL and SCGL distributions are shown. The linear plots elucidate density dynamics and enable comparisons with the parent Lindley model, whilst the circular plots present an intuitive visualization for directed or periodic data. Collectively, these graphical representations enhance comprehension of the suggested models' flexibility and application.

3.1 Linear and Circular Representations of the WGL Distribution

The PDF curves of the WGL distribution are depicted in linear and circular formats, as shown in Figure 1 and Figure 2, respectively. To ensure consistency, both figures are produced under identical parameter configurations: the first two examples pertain to $\lambda < \alpha$, the third and fourth cases pertain to $\lambda > \alpha$, and the last two cases pertain to the specific condition when $\lambda = \alpha$. This structured comparison elucidates the impact of parameter relationships on the overall form and dynamics of the WGL distribution in both linear and circular forms.

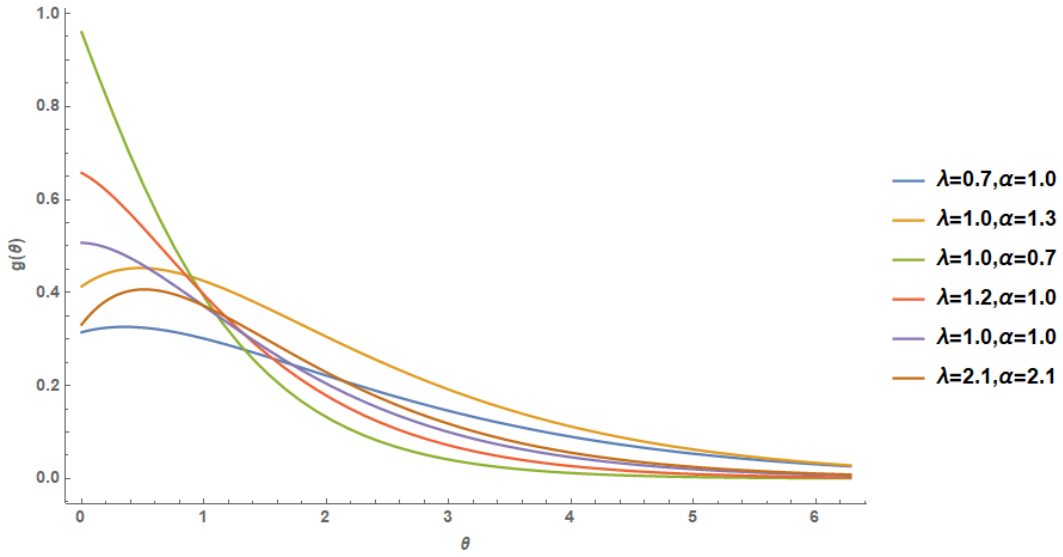

Fig. 1: Linear representation of WGL distribution.

In Figure 1, the linear representation provides an intuitive view of how the density varies over the positive real line. When $\lambda < \alpha$, the distribution is more spread out with heavier tails, while for $\lambda > \alpha$, the distribution becomes more concentrated around smaller values of the random variable. The special case $\lambda = \alpha$ produces an intermediate form, balancing between spread and concentration. On the other hand, Figure 2 presents the circular representation of the same distribution, obtained by wrapping the density around the circumference of the unit circle. This visualization emphasizes the periodic nature of the WGL distribution and provides insight into how probability mass is distributed across angular directions. The circular plots highlight that parameter settings not only influence the skewness and concentration but also the clustering of probability mass along particular angular regions. Together, these figures demonstrate how the WGL distribution can be interpreted in both traditional (linear) and directional (circular) contexts, showcasing its flexibility in modeling datasets where either representation is required.

© 2026 NSP
Natural Sciences Publishing Cor.

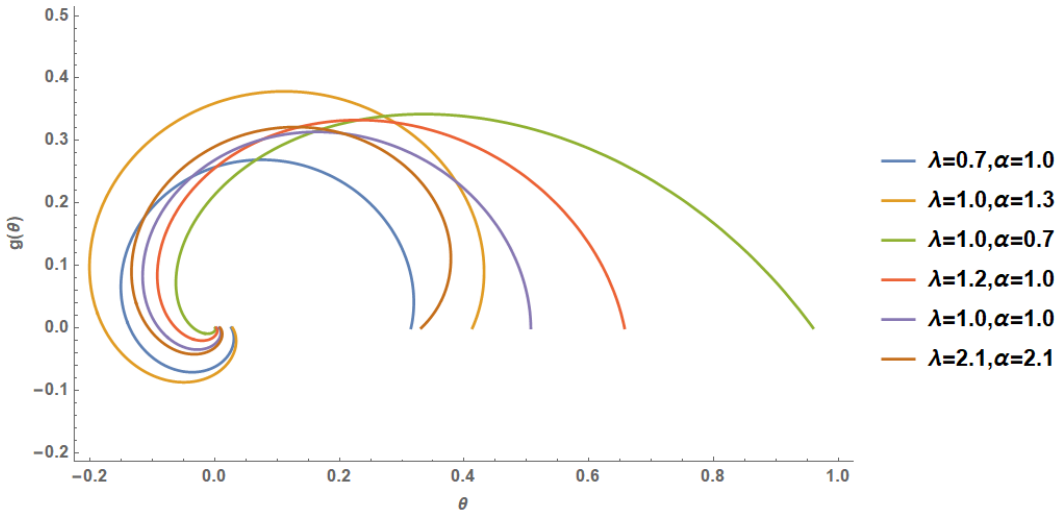

Fig. 2: Circular representation of WGL distribution.

3.2 Linear and Circular Representations of SCGL Distribution

Correspondingly, the PDF curves of the SCGL distribution are presented in Figures 3 and 4, representing the linear and circular cases, respectively. The linear representation in Figure 3 reveals how the SCGL distribution extends the flexibility of the generalized Lindley model to semi-circular data. Similar to the WGL case, variations in the relationship between the parameters λ and α influence the skewness, concentration, and spread of the distribution. When $\lambda < \alpha$, the curves tend to display heavier right tails, while for $\lambda > \alpha$, the density becomes more peaked around smaller values. The balance observed in the case of $\lambda = \alpha$ reflects a transitional shape that lies between these two extremes. In contrast, Figure 4 highlights the circular behavior of the SCGL distribution obtained through the inverse stereographic projection (ISP) method. Unlike the wrapped case, the semi-circular nature is evident in these plots, where probability mass is restricted to semi-arcs on the circle. This behavior is particularly important for datasets that exhibit directional tendencies confined to half a cycle, such as phenomena with inherent polarity, preferred orientations, or temporal events occurring over a restricted interval of a full rotation.

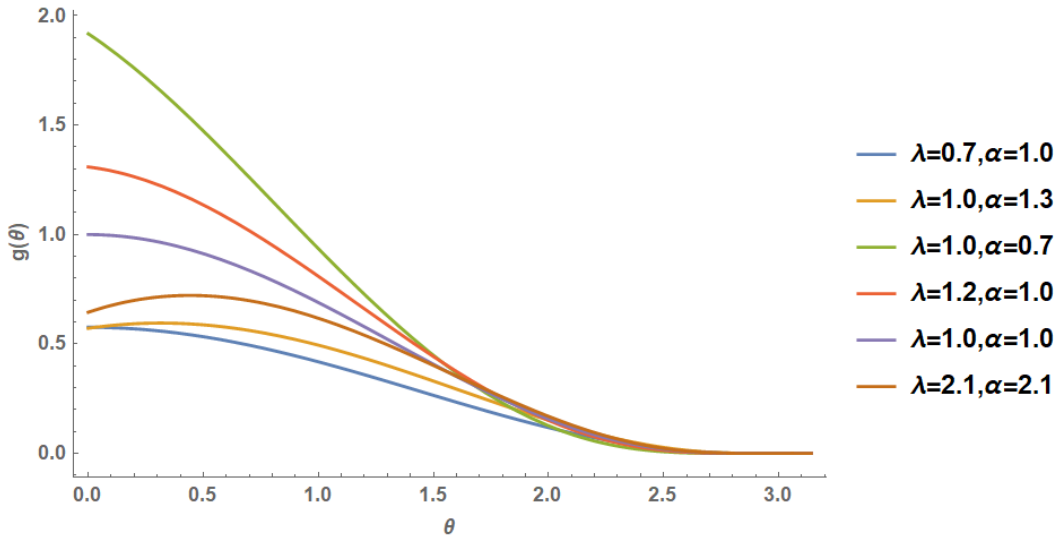

Fig. 3: Linear representation of SCGL distribution.

© 2026 NSP
Natural Sciences Publishing Cor.

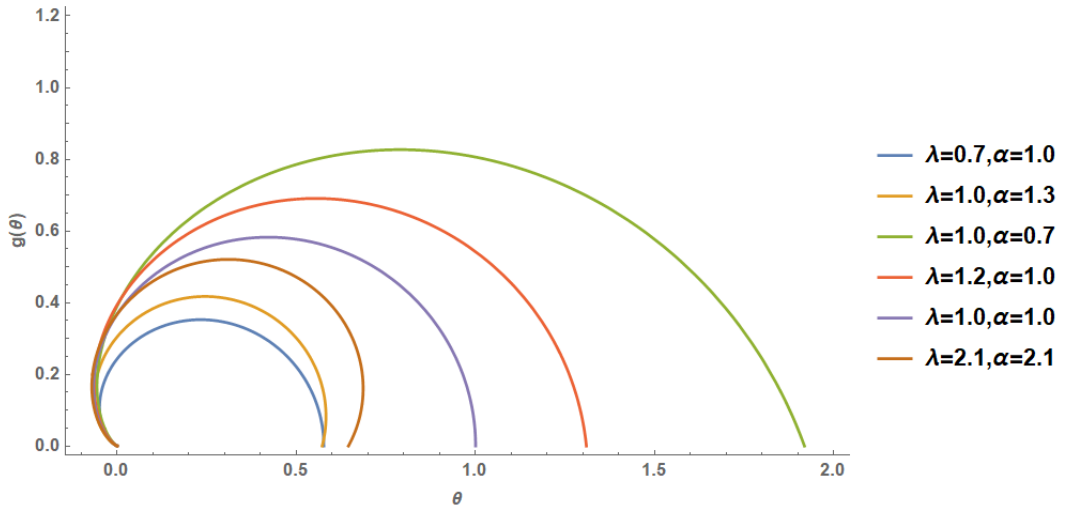

Fig. 4: Circular representation of SCGL distribution.

From a modeling standpoint, the SCGL distribution offers a superior match in scenarios where the data inherently exhibit semi-circular patterns. It is particularly effective for simulating orientations or temporal events that are confined to a small semicircular range rather than encompassing the entire circle. The subsequent comparison analysis demonstrates that SCGL frequently identifies such patterns more efficiently than its circular equivalent (WGL), which allocates mass uniformly over the entire circumference. Consequently, Figures 3 and 4 not only depict the theoretical density curves of SCGL but also highlight its prospective practical benefits in real-world data fitting, particularly in scenarios where semi-circular properties predominate the dataset's structure.

4 Trigonometric Moments and Characteristic Functions of WGL and SCGL Distributions

This section focuses on the characteristic functions of the WGL and SCGL distributions, along with their associated trigonometric moments. The characteristic function plays a central role in probability theory, as it uniquely characterizes the distribution and provides a bridge to obtaining moments, dependence measures, and properties that are essential in data modeling. Table 1 summarizes the closed-form expressions of the characteristic functions for both distributions.

Table 1: Characteristic functions of WGL and SCGL distributions.

Sl. No.	Distribution	Characteristic Function
1	WGL	$\varphi(p)=\frac{\lambda^2}{\alpha(\lambda+\alpha^2)}\left[\frac{\frac{\lambda}{\alpha}-\alpha-ip}{(\frac{\lambda}{\alpha}-ip)^2}\right]$
2	SCGL	$\phi(\theta)=\frac{\lambda^2}{\alpha(\lambda+\alpha^2)}\int_0^{\pi}\left(\frac{1}{1+\cos\theta}\right)\left\{1+\alpha\tan\left(\frac{\theta}{2}\right)\right\}e^{-\frac{\lambda}{\alpha}\tan\left(\frac{\theta}{2}\right)}e^{ip\theta}d(\theta)$

Since both WGL and SCGL are circular-type distributions, their properties are naturally studied through trigonometric moments. By definition, the p^{th} trigonometric moment is given as

$$\Phi_p=\alpha_p+i\beta_p;\quad p=\pm1,\pm2,\ldots,$$

where α_p and β_p represent the cosine and sine moments, respectively. These components provide direct insights into the distribution?s mean direction, concentration, and shape. Specifically, they can be expressed as

$$\alpha_p=\rho_p\cos\mu_p,\quad \beta_p=\rho_p\sin\mu_p,$$

© 2026 NSP
Natural Sciences Publishing Cor.

where μ_p denotes the mean direction and ρ_p the resultant length (a measure of concentration). Now, the central trigonometric moments are

$$\bar{\alpha}_p = \rho_p \, cos(\mu_p - p\mu_1) \;\text{ and }\; \bar{\beta}_p = \rho_p \, sin(\mu_p - p\mu_1)$$

The non-central trigonometric moments for the WGL distribution can be obtained explicitly, leading to useful measures such as mean direction, circular variance, skewness, and kurtosis. These measures are tabulated in Table 2. For instance, the resultant length ρ quantifies how strongly the data clusters around the mean direction: a value close to 1 indicates high concentration, while values near 0 suggest dispersion across the circle. Similarly, skewness and kurtosis allow us to capture asymmetry and tail behavior, crucial in applications such as wind direction modeling, navigation, or biological cycle data.

Table 2: Population characteristics of WGL distribution.

Sl. No.	Measure	WGL
1	Mean Direction	$\mu = \arctan\left\{2\left(\frac{\alpha}{\lambda}\right) - \left(\frac{\alpha}{\lambda-\alpha^2}\right)\right\}$
2	Resultant Length	$\rho = \frac{\lambda^2\left\{\left(\frac{\lambda}{\alpha}-\alpha\right)^2+1\right\}^{-\frac{1}{2}}}{\alpha(\lambda+\alpha^2)\left\{\left(\frac{\lambda}{\alpha}\right)^2+1\right\}^{-1}}$
3	Circular Variance	$V_0 = 1-\rho$
4	Skewness	ξ_1^0
5	Kurtosis	ξ_2^0

The skewness $\xi_1^0 = \frac{\bar{\beta}_2}{V_0^{\frac{3}{2}}}$ and kurtosis $\xi_2^0 = \frac{\bar{\alpha}_2-(1-V_0)^4}{V_0^2}$ of the WGL model can be listed as

$$\xi_1^0 = \frac{\left(\frac{\lambda^2\left\{\left(\frac{\lambda}{\alpha}-\alpha\right)^2+4\right\}^{-\frac{1}{2}}}{\alpha(\lambda+\alpha^2)\left\{\left(\frac{\lambda}{\alpha}\right)^2+4\right\}^{-1}}\right)\sin\left[\arctan\left(2\left(\frac{2\alpha}{\lambda}-\frac{\alpha}{\lambda-\alpha^2}\right)\right)-2\arctan\left(\frac{2\alpha}{\lambda}-\frac{\alpha}{\lambda-\alpha^2}\right)\right]}{\left(1-\frac{\lambda^2\left\{\left(\frac{\lambda}{\alpha}-\alpha\right)^2+1\right\}^{-\frac{1}{2}}}{\alpha(\lambda+\alpha^2)\left\{\left(\frac{\lambda}{\alpha}\right)^2+1\right\}^{-1}}\right)^{\frac{3}{2}}}$$

and

$$\xi_2^0 = \frac{r\cos\left\{2\arctan\left(\frac{2\alpha}{\lambda}\right)-\arctan\left(\frac{2}{\frac{\lambda}{\alpha}-\alpha}\right)-2\left[2\arctan\left(\frac{\alpha}{\lambda}\right)-\arctan\left(\frac{1}{\frac{\lambda}{\alpha}-\alpha}\right)\right]\right\}-s^4}{(1-s)^2}$$

where

$$r = \frac{\lambda^2\left\{\left(\frac{\lambda}{\alpha}-\alpha\right)^2+4\right\}^{-1/2}}{\alpha(\lambda+\alpha^2)\left\{\left(\frac{\lambda}{\alpha}\right)^2+4\right\}^{-1}} \quad\text{and}\quad s = \frac{\lambda^2\left\{\left(\frac{\lambda}{\alpha}-\alpha\right)^2+1\right\}^{-1/2}}{\alpha(\lambda+\alpha^2)\left\{\left(\frac{\lambda}{\alpha}\right)^2+1\right\}^{-1}}.$$

© 2026 NSP
Natural Sciences Publishing Cor.

For the SCGL distribution, trigonometric moments are instead derived through integrals involving the semi-circular support. The first-order moments α_1 and β_1 form the basis for calculating higher-order properties, as shown below:

$$\alpha_1 = \int_0^{\pi} \cos(\theta)\, m(\theta) d\theta, \qquad \beta_1 = \int_0^{\pi} \sin(\theta)\, m(\theta) d\theta,$$

with analogous expressions for higher-order moments. Using these results, population characteristics of SCGL distribution are listed in Table 3. These demographic attributes are not merely theoretical entities but also offer pragmatic

Table 3: Population characteristics of SCGL distribution.

Sl. No.	Measure	SCGL
1	Mean Direction	$\mu = \tan^{-1}\left(\frac{\beta_1}{\alpha_1}\right)$
2	Resultant Length	$\rho = \sqrt{\alpha_1^2 + \beta_1^2}$
3	Circular Variance	$v = 1 - \rho$
4	Skewness	$\gamma_1 = \frac{\beta_2^*}{(1-\rho)^{\frac{3}{2}}}$
5	Kurtosis	$\gamma_2 = \frac{\alpha_2^* - \rho^4}{(1-\rho)^2}$

direction for data modeling. The mean direction signifies the primary orientation in directional datasets; the resultant length and variance facilitate the evaluation of concentration, crucial for differentiating between densely clustered and broadly dispersed circular data; skewness and kurtosis provide further understanding of asymmetry and peakedness, important for model fitting and hypothesis testing in practical applications. Consequently, the examination of characteristic functions and trigonometric moments provides researchers with an effective arsenal for fitting the WGL and SCGL models to empirical datasets, regardless of their adherence to circular or semi-circular patterns. These distributions are particularly pertinent to practical disciplines such as environmental science, biology, geology, and engineering, where cyclical or semi-cyclical data commonly occur.

5 Data Analysis: Model Fitting, Goodness-of-Fit Assessment, Visualization, and Informed Decision-Making

In this section, the proposed WGL distribution is fitted to two real-life datasets to evaluate its goodness-of-fit. The WGL distribution is compared with several competing distributions, including the wrapped Lindley (WL), wrapped modified Lindley (WML), and wrapped XLindley (WXL) distributions.

5.1 Dataset I: Movement of Turtles

The dataset under consideration records the directional movements or orientations of 76 turtles after laying eggs, as reported in [9]. Each observation represents the angle in degrees measured clockwise from the north. The circular visualization of these directional data is presented in Figure 5, which provides an intuitive understanding of the turtles? movement patterns around the nest sites. In Table 4, we have presented five different comparison measures used as selection criteria for all these distributions, such as negative log-likelihood value (-L), Akaike Information Criterion (AIC), Consistent Akaike Information Criterion (CAIC), Bayesian Information Criterion (BIC), Hannan-Quinn Information Criterion (HQIC). In general, the better fit of the distribution corresponds to the smaller value of the statistics such as -L, AIC, CAIC, BIC and HQIC. Considering the values of these measures, it is clear that the WGL distribution is the most appropriate distribution as compared to the other three distributions. Figure 6 presents the density functions and distribution functions estimated by WGL, WL, WML and WXL distributions. Figure 7 shows P-P plots that represent the empirical cumulative versus estimated cumulative functions of the WGL, WL, WML and WXL distributions.

© 2026 NSP
Natural Sciences Publishing Cor.

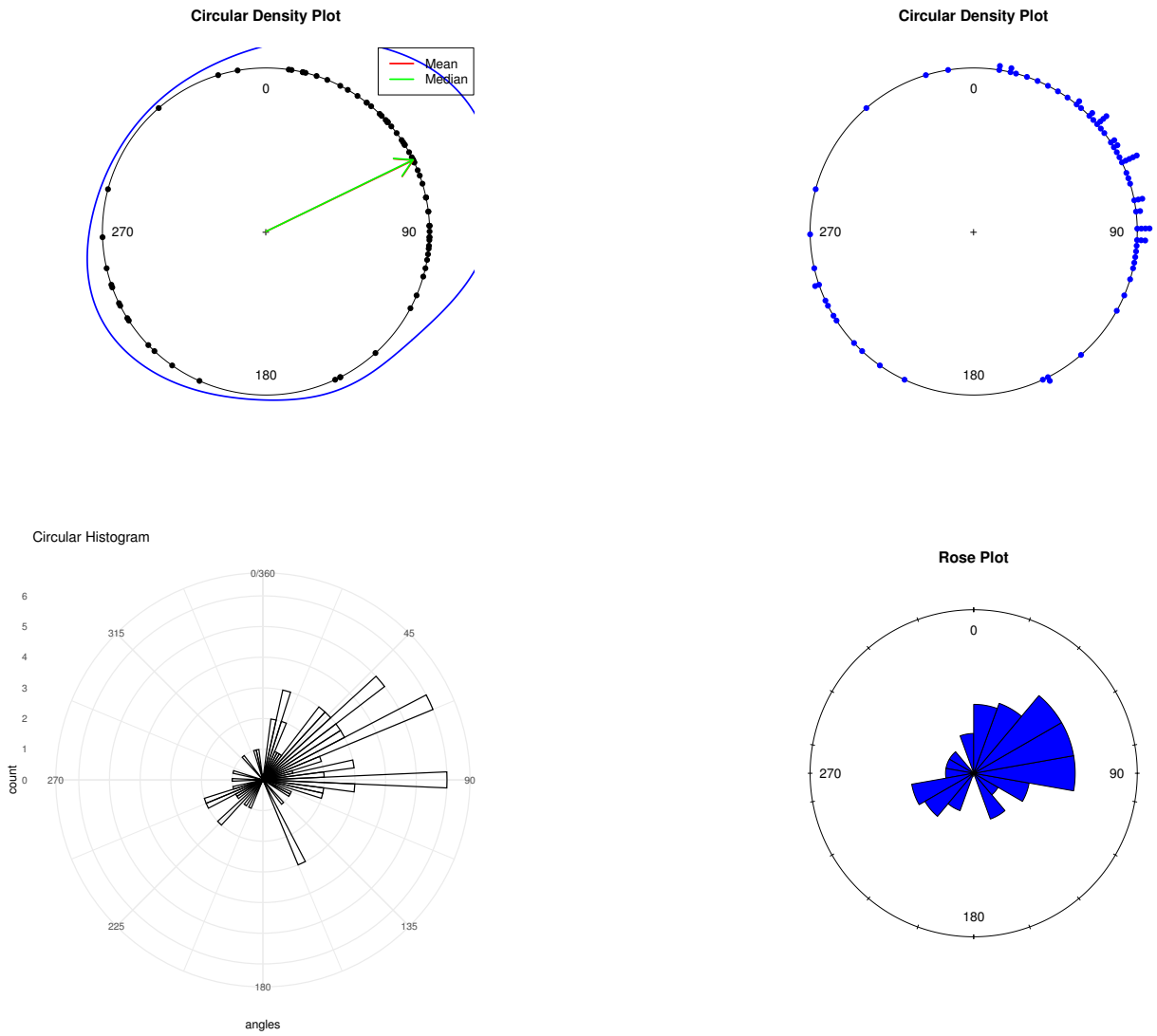

Fig. 5: Circular plots of dataset I.

Table 4: The goodness-of-fit measures for tested distributions based on dataset I.

Distribution	MLE	-L	AIC	CAIC	BIC	HQIC
WGL	$\lambda = 0.38317$ $\alpha = 0.82939$	113.312	230.623	230.788	235.285	232.486
WL	λ =0.97268	124.378	250.755	250.809	253.086	251.687
WML	λ =0.40943	121.382	244.765	244.819	247.095	245.696
WXL	λ =0.736428	124.387	250.773	250.827	253.104	251.705

5.2 Dataset II: Wind Directions

The second dataset consists of wind direction measurements in degrees recorded at Gorleston, England, between 11 a.m. and 12 noon on Sundays throughout 1968, covering all four seasons, as reported in [8]. Figure 8 presents the circular plot of the wind direction data, which visually represents the distribution of wind orientations and facilitates the analysis of seasonal patterns.

© 2026 NSP
Natural Sciences Publishing Cor.

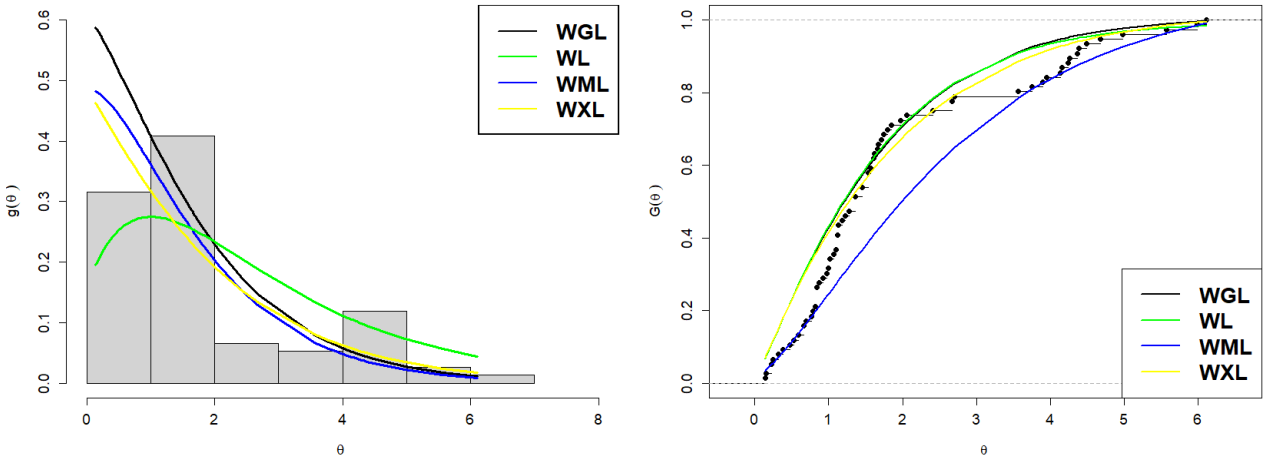

(a) **(b)**

Fig. 6: The fitted PDF and CDF of the tested models for dataset I.

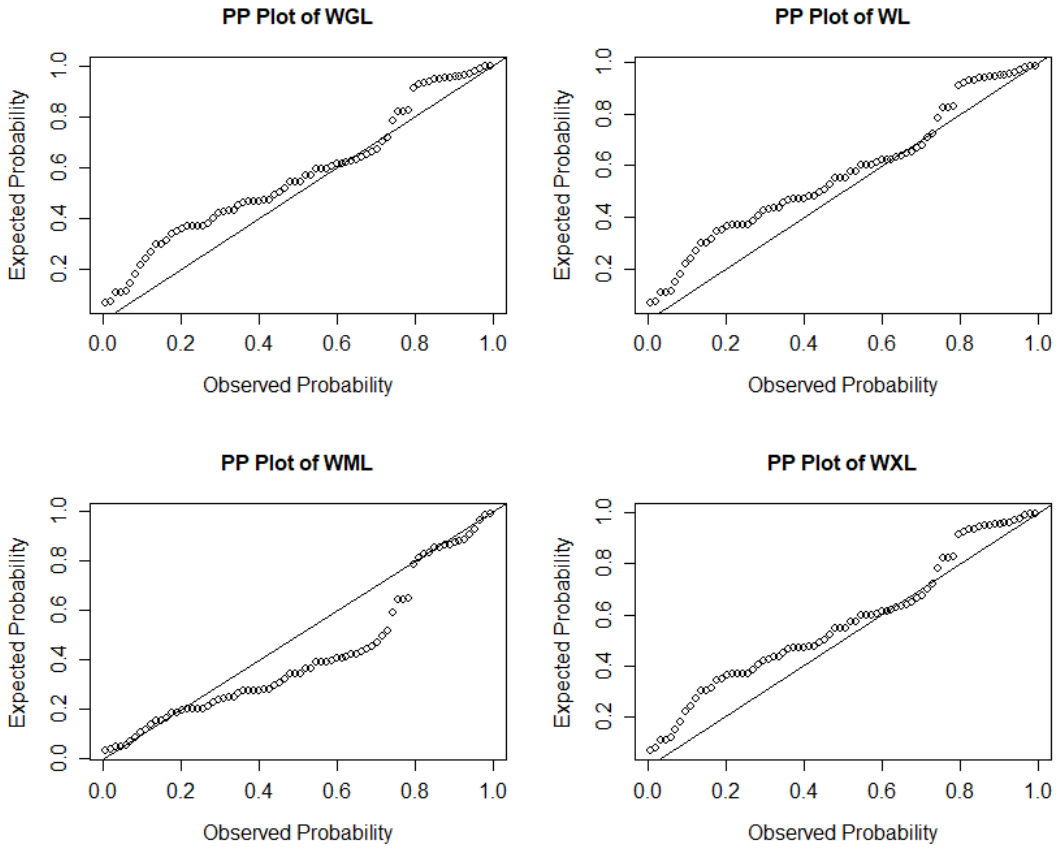

Fig. 7: The P-P plots for tested distributions based on dataset I.

© 2026 NSP
Natural Sciences Publishing Cor.

From Table 5, we can observe that the values of -L, AIC, CAIC, BIC and HQIC are the least for WGL distribution as compared to WL, WML and WXL distributions, which satisfy the conditions for the better fit of the distributions. Figure 9 presents the density functions and distribution functions estimated by WGL, WL, WML and WXL distributions and Figure 10 shows P-P plots that represent the empirical cumulative versus estimated cumulative functions of the WGL, WL, WML and WXL distributions for the wind direction data.

Table 5: The goodness-of-fit measures for tested distributions based on dataset II.

Distribution	MLE	-L	AIC	CAIC	BIC	HQIC
WGL	$\lambda = 0.38317$ $\alpha = 0.82939$	87.384	178.769	179.029	182.552	180.204
WL	λ =0.58942	112.987	227.974	228.059	229.866	228.692
WML	$\lambda = 0.29380$	93.9507	189.902	189.987	191.793	190.619
WXL	$\lambda = 0.45427$	107.050	216.100	216.185	217.992	216.818

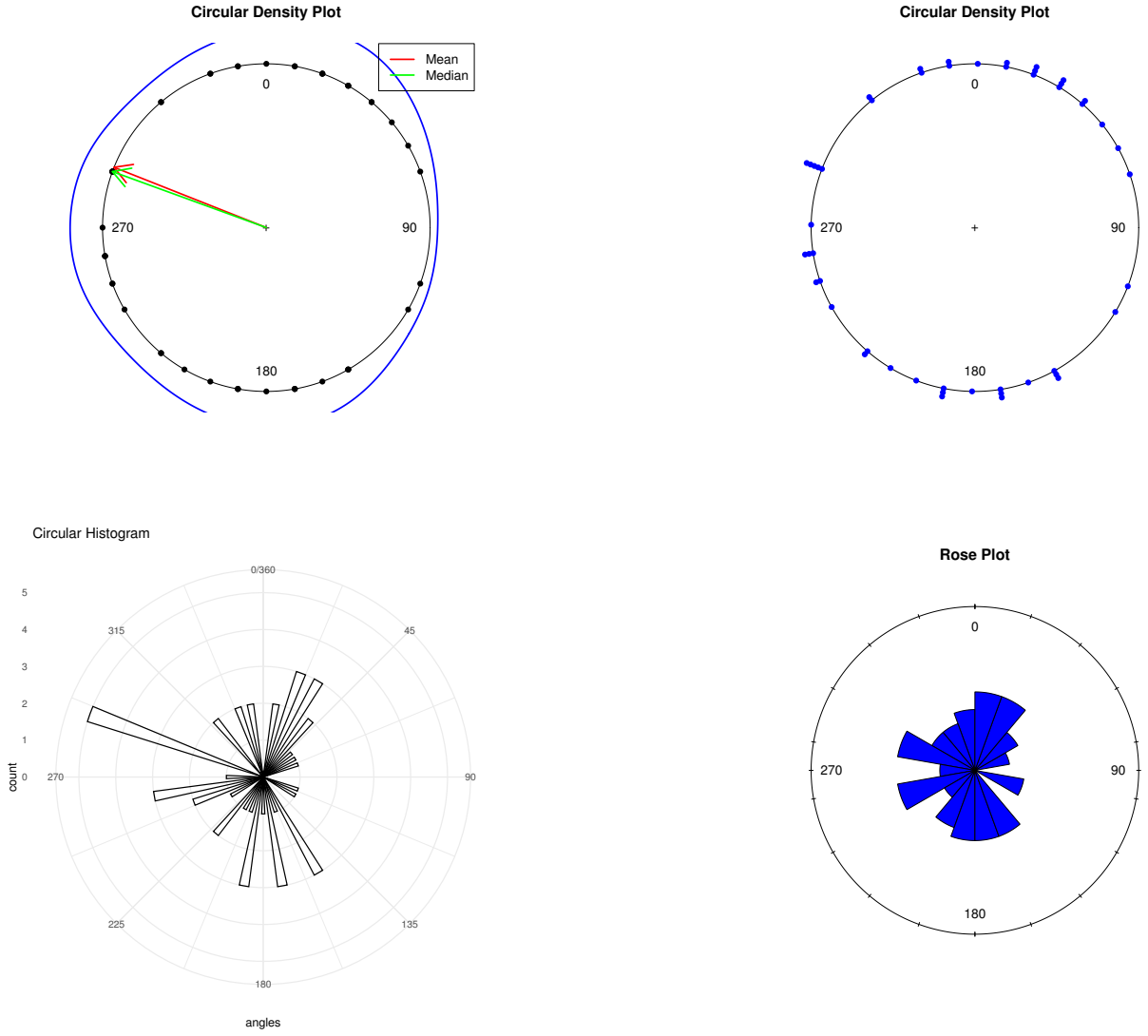

Fig. 8: Circular plots of dataset II.

© 2026 NSP
Natural Sciences Publishing Cor.

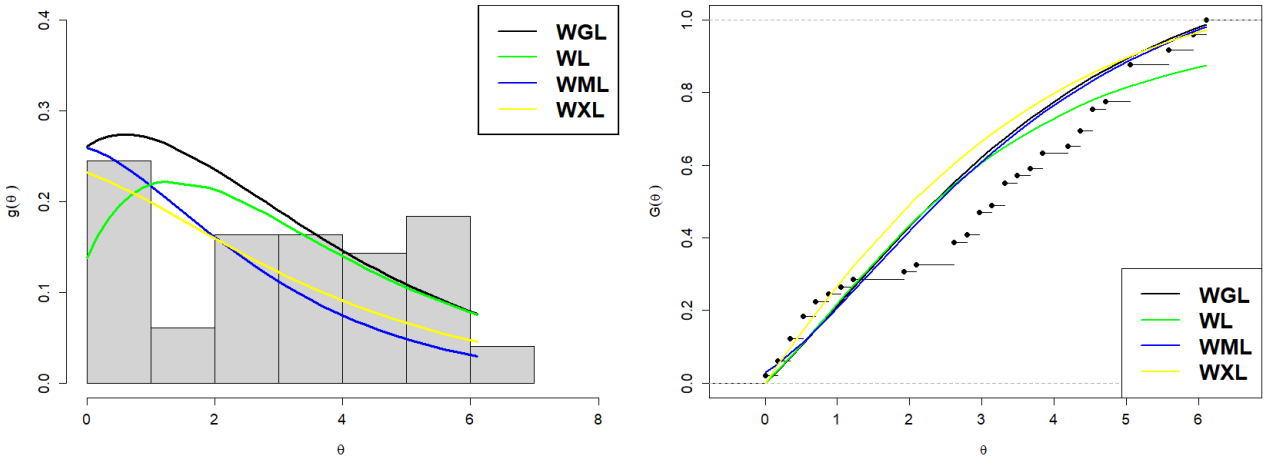

(a) **(b)**

Fig. 9: The fitted PDF and CDF of tested models for dataset II.

6 Comparative Study on WGL and SCGL Distributions

This section examines two real-world datasets to assess the applicability and select the more suitable distribution between the WGL and SCGL models. Both datasets exhibit a semi-circular nature, as the semi-circular distribution, specifically the SCGL distribution, is inadequate for managing complete circular data where data points span from 0 to 2π. The circular plots for both datasets illustrate that the data originates from a semi-circular distribution. The performance of the WGL and SCGL distributions is evaluated using multiple model selection criteria, including -L, AIC, CAIC, BIC, and HQIC, to identify the optimal model.

6.1 Dataset III: Feldspar Laths in Basalt

The collection comprises measurements of the long-axis orientation of 60 feldspar laths in basalt [7]. [18] demonstrated the applicability of axial normal distribution in environmental and ecological sciences utilizing this dataset.

Figure 11 depicts the circular plot, which distinctly indicates that the observed angles are primarily concentrated in the first and second quadrants. This pattern verifies that the data align with a half-circular distribution, where the angle $\theta \in (0, \pi]$. The concentration of angles indicates a natural asymmetry in orientations, underscoring the importance of modeling the data with semi-circular distributions. Table 6 presents the goodness-of-fit metrics, comprising the -L, AIC, CAIC, BIC, and HQIC, for both the WGL and SCGL distributions. The SCGL distribution demonstrates lower values across all statistics, signifying a more favorable match relative to the WGL distribution. This outcome substantiates the assertion that the semi-circular SCGL distribution is more suitable for modeling.

Table 6: The goodness-of-fit measures of WGL and SCGL distributions for dataset III.

Distribution	MLE	-L	AIC	CAIC	BIC	HQIC
WGL	$\alpha = 0.74999$ $\lambda = 0.58156$	73.0963	150.193	150.403	154.381	151.831
SCGL	$\alpha = 1.46974$ $\lambda = 1.50621$	1.09786	6.19572	6.40625	10.3844	7.83415

© 2026 NSP
Natural Sciences Publishing Cor.

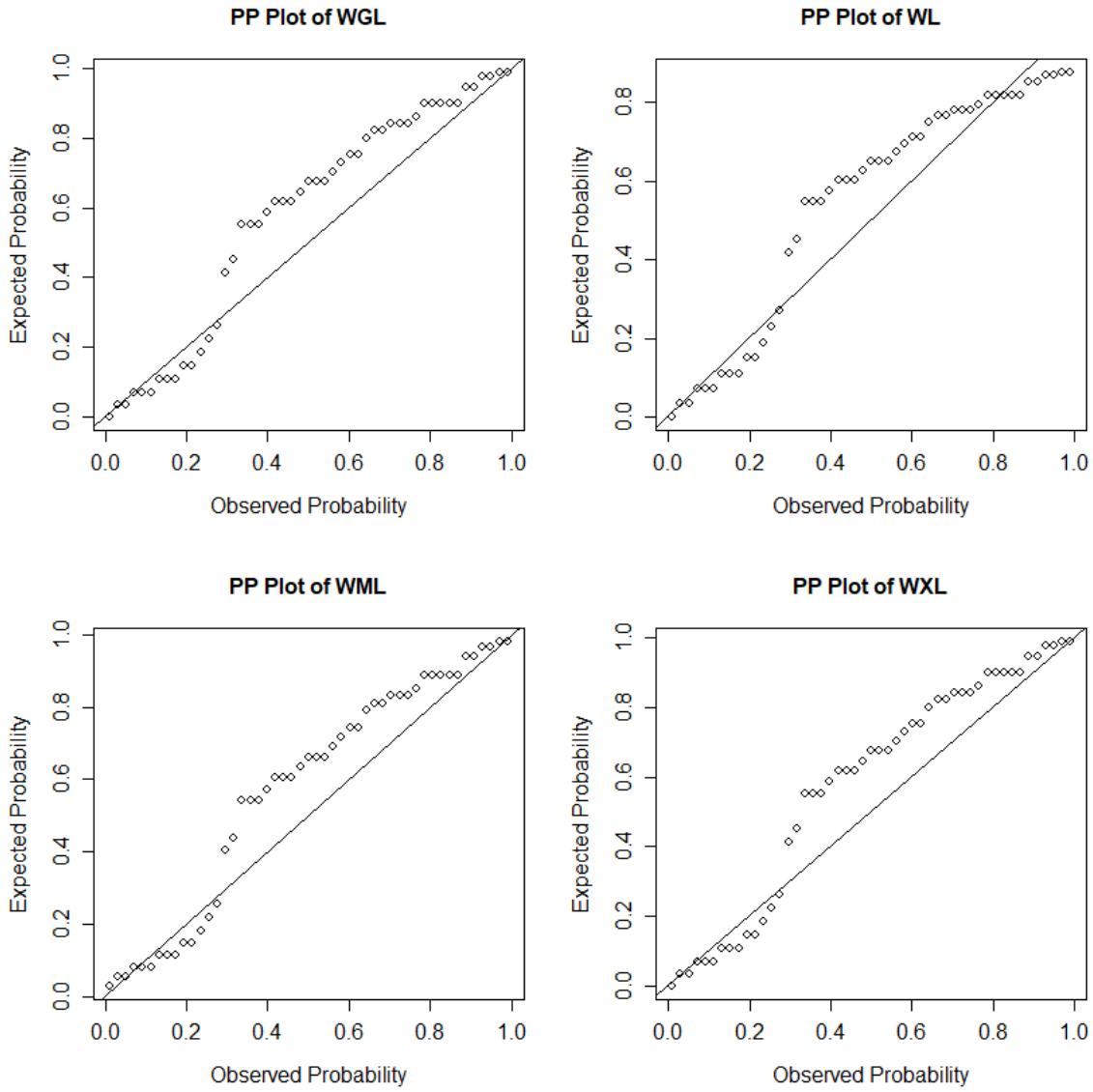

Fig. 10: The P-P plots of tested distributions for dataset II.

6.2 Dataset IV: Measurements of Median Direction

The dataset comprises 63 measurements of median face-cleat directions recorded at 20-meter intervals along a tunnel in the Wallsend Borehole Colliery, NSW, Australia [7]. The variations in the orientations of face-cleats are significant indicators of potential hazardous mining circumstances, rendering precise modeling of the directional data essential for risk assessment and decision-making. The 63 measurements were analyzed by fitting both WGL and SCGL distributions.

Figure 13 illustrates the circular plot of the dataset, demonstrating that the observations are primarily concentrated in the first and second quadrants. This concentration suggests that the data align with a semi-circular distribution, with $\theta \in (0, \pi]$, underscoring the possible benefits of employing a semi-circular model instead of a fully circular one. The numerical outcomes of the model selection criteria, encompassing the -L, AIC, CAIC, BIC, and HQIC, are consolidated in Table 7. The table clearly indicates that the SCGL distribution surpasses the WGL distribution, attaining the lowest values in all selection criteria. This offers robust quantitative support for the SCGL hypothesis concerning this dataset. Furthermore, Figure 14 illustrates the histogram of face-cleat orientations superimposed with the fitted probability density functions of both WGL and SCGL distributions. The histogram clearly validates the enhanced alignment of the SCGL

© 2026 NSP
Natural Sciences Publishing Cor.

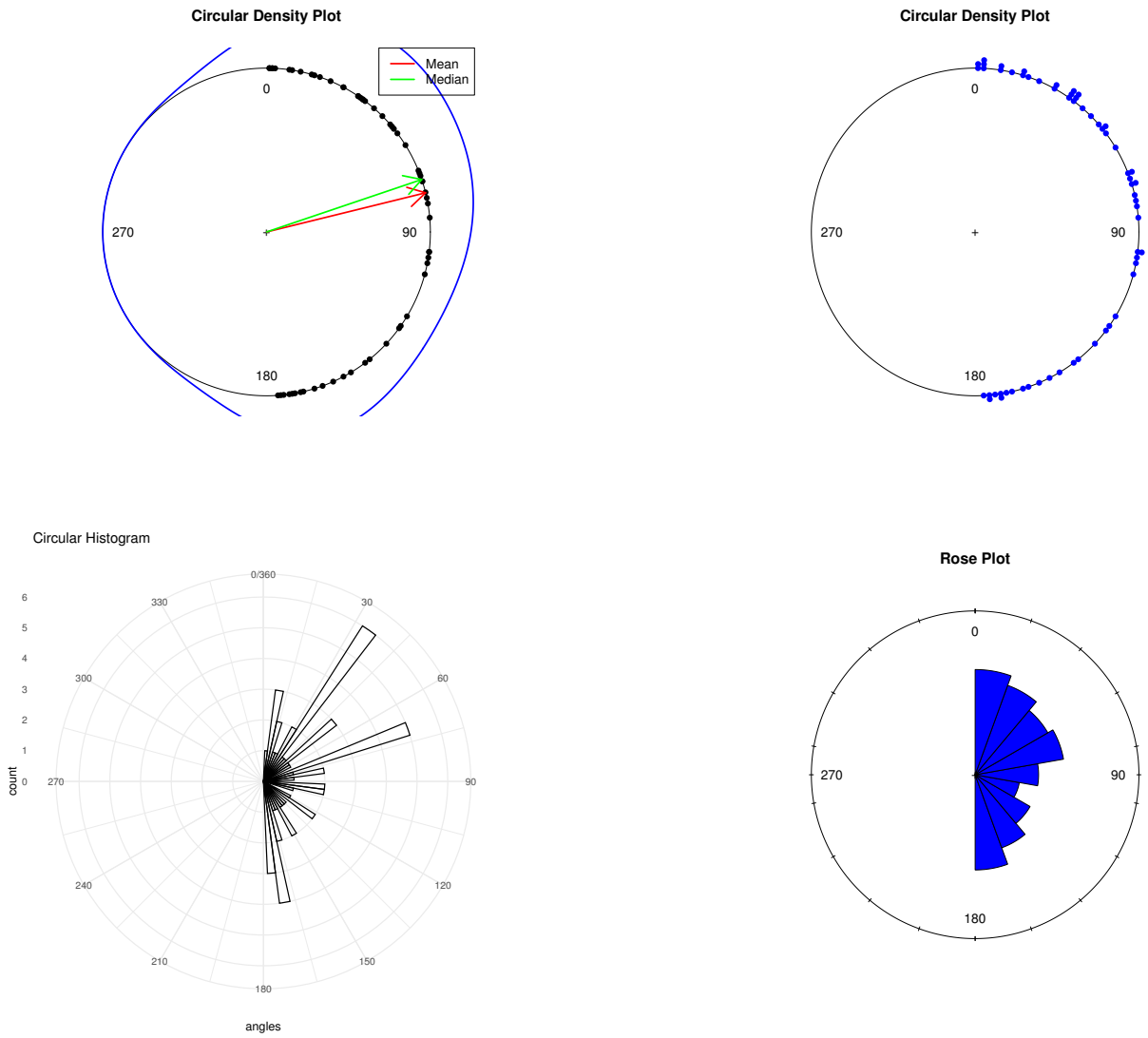

Fig. 11: Circular plots of dataset III.

density function with the empirical data, particularly in its ability to capture skewness and angle concentration. Both the numerical assessment in Table 7 and the visual analysis in Figure 14 indicate that the SCGL distribution offers the optimal match for the median face-cleat orientations in this dataset. This understanding is essential for informed decision-making in mining operations, enabling a more precise evaluation of directional trends and potential hazards.

Table 7: The goodness-of-fit measures of WGL and SCGL distributions for dataset IV.

Distribution	MLE	-L	AIC	CAIC	BIC	HQIC
WGL	$\alpha = 1.48489$ $\lambda = 0.99996$	18.9399	33.8799	33.6799	29.5936	32.1941
SCGL	$\alpha = 1.50901$ $\lambda = 0.60819$	9.82018	23.6404	23.8404	27.9266	25.3262

© 2026 NSP
Natural Sciences Publishing Cor.

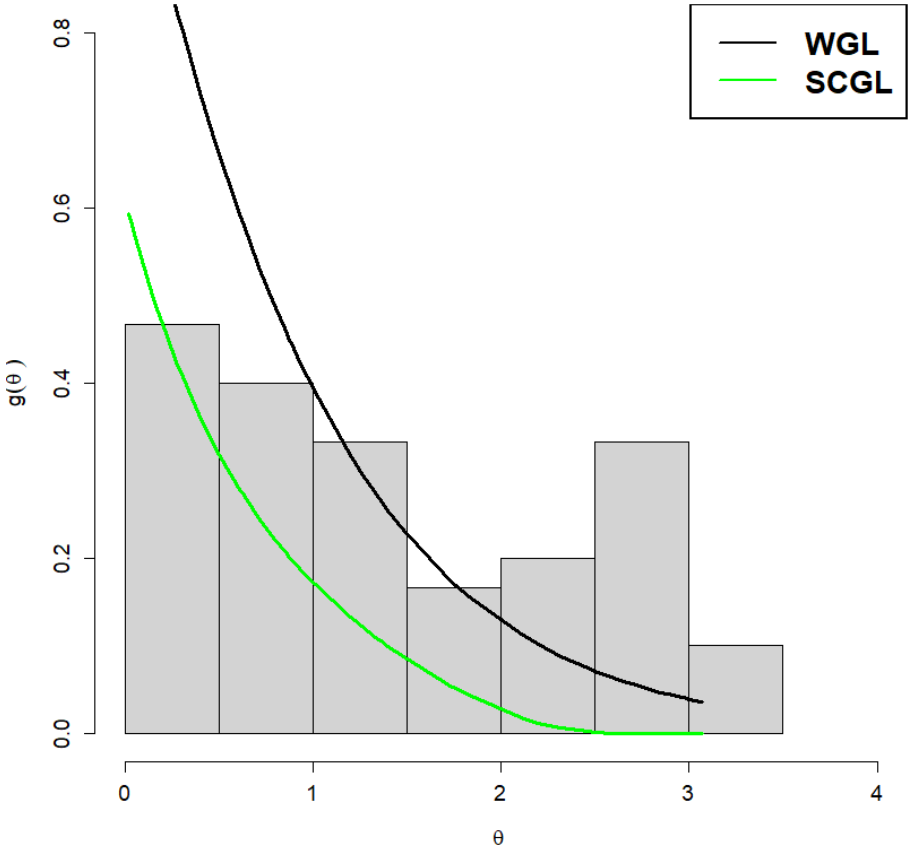

Fig. 12: The fitted PDF of WGL and SCGL distributions for dataset III.

7 Conclusions

This study utilized the GL distribution to develop a novel circular distribution, termed the WGL distribution, and a new semi-circular distribution, designated as the SCGL distribution, employing the ISP approach. A thorough comparison examination of the WGL and SCGL distributions was conducted. The PDFs and CDFs of both distributions were generated and analyzed, supplemented with comprehensive graphical representations that illustrated their behavior across varying parameter values. The characteristic functions and trigonometric moments of WGL and SCGL distributions, together with associated statistical aspects, were organized in tabular format to enhance comprehension of their distributional attributes. Four real-world semi-circular datasets were investigated to assess the practical applicability and goodness-of-fit of these distributions. The datasets comprised directional measurements, including turtle movements, orientations of feldspar laths, and median directions of face-cleats, which were appropriate for evaluating both circular and semi-circular models. The comprehensive fitting results indicated that the SCGL distribution regularly surpassed the WGL distribution in both numerical selection criteria (negative log-likelihood, AIC, CAIC, BIC, HQIC) and visual assessment of fitted PDFs and CDFs. The anticipated higher performance is attributable to the datasets, which were sourced from random samples of semi-circular distributions, where $\theta \in (0, \pi]$. The results indicated that SCGL was better suitable for modeling semi-circular data, while WGL offered a satisfactory approximation for entirely circular data. The scope of this research can be expanded in other areas for future investigation. The advancement of multivariate expansions of the WGL and SCGL distributions may facilitate the modeling of dependent angular data in environmental, biological, and engineering contexts. Secondly, additional research might investigate the integration of covariate information into circular and semi-circular regression models utilizing these distributions. Ultimately, computational procedures for parameter estimation

© 2026 NSP
Natural Sciences Publishing Cor.

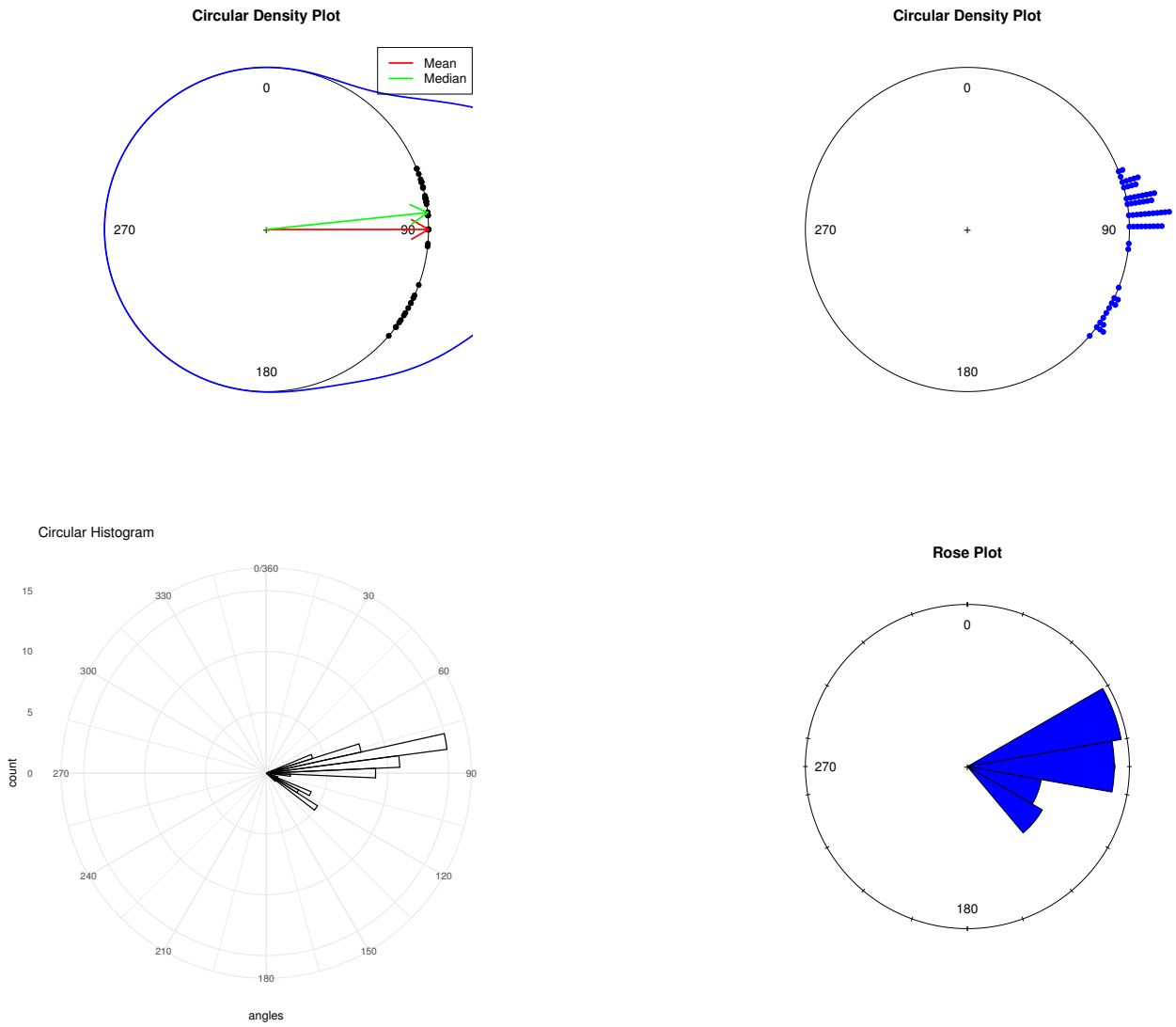

Fig. 13: Circular plots of dataset IV.

under censored or truncated conditions can be formulated, thereby augmenting the practical applicability of the proposed distributions in intricate real-world situations.

Data Availability

The dataset used in this study is secondary data and has been clearly cited in the manuscript.

Conflict of Interest

The authors declare that they have no conflicts of interest.

© 2026 NSP
Natural Sciences Publishing Cor.

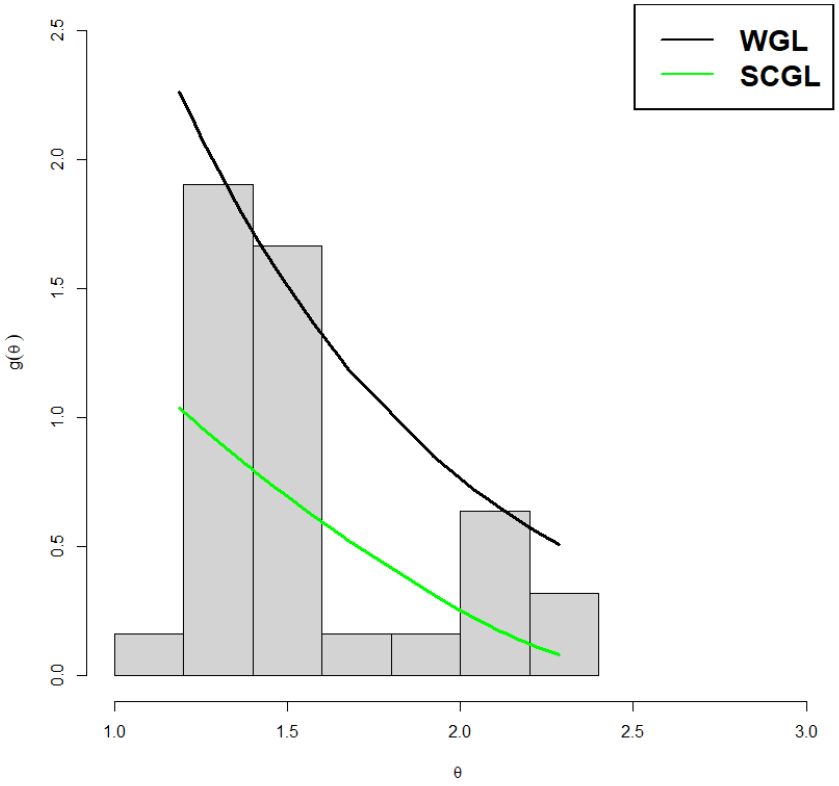

Fig. 14: The fitted PDF of WGL and SCGL distributions for dataset IV.

Abbreviations

The following abbreviations are used in this manuscript:

WGL	:	Wrapped Generalized Lindley
SCGL	:	Semi-Circular Generalized Lindley
PDF	:	Probability Density Function
CDF	:	Cumulative Distribution Function
WL	:	Wrapped Lindley
WML	:	Wrapped Modified Lindley
WXL	:	Wrapped XLindley
AIC	:	Akaike Information Criterion
CAIC	:	Consistent Akaike Information Criterion
BIC	:	Bayesian Information Criterion
HQIC	:	Hannan-Quinn Information Criterion
MLE	:	Maximum Likelihood Estimation

References

[1] Mardia, K.V. *Statistics of Directional Data*, Academic Press, London, 1972.
[2] Von Mises, R. On the integrity of atomic weights and related questions. *Physical Journal*, **19**, 490-500 (1918).
[3] Fisher, R.A. Dispersion on a sphere. *Proceedings of the Royal Society of London A* **217(1130)**, 295-305 (1953).

© 2026 NSP
Natural Sciences Publishing Cor.

[4] Greenwood, J.A., Durand, D. The distribution of length and components of the sum of n random unit vectors. *Annals of Mathematical Statistics* **26(2)**, 233-246 (1955).
[5] Watson, G.S., Williams, E.J. On the construction of significance tests on the circle and the sphere. *Biometrika* **43**, 344-352 (1956).
[6] Stephens, M.A. Techniques for directional data. *Technical Report No. 150, Department of Statistics, Stanford University*.
[7] Fisher, N.I. *Statistical Analysis of Circular Data*, Cambridge University Press, 1993.
[8] Mardia, K.V., Jupp, P.E. *Directional Statistics*, Wiley, Chichester, 2000.
[9] Jammalamadaka, S.R., SenGupta, A. *Topics in Circular Statistics*, World Scientific, Vol. 5, 2001.
[10] SenGupta, A., Arnold, B.C. *Directional Statistics for Innovative Applications: A Bicentennial Tribute to Florence Nightingale*, Springer Nature, Singapore, 2022.
[11] Kumar, S., Arnold, B.C., Shimizu, K., Laha, A.K. *Directional and Multivariate Statistics*, Springer Nature, Singapore, 2025.
[12] Lévy, P.L. Addition of random variables defined on a circumference. *Bulletin of the Mathematical Society of France* **67**, 1-41 (1939).
[13] Gatto, R., Jammalamadaka, S.R. Inference for wrapped α-stable circular models. *Sankhya* **65(2)**, 333-355 (2003).
[14] Joshi, S., Jose, K.K. Wrapped Lindley distribution. *Communications in Statistics?Theory and Methods* **47(5)**, 1013-1021 (2018).
[15] Bell, W., Nadarajah, S. A review of wrapped distributions for circular data. *Mathematics* **12(16)**, 2440 (2024).
[16] Sakthivel, K.M., Mathew, A. Modelling directional data with wrapped Chris-Jerry distribution in geological and medical domains. *Advances and Applications in Statistics* **92(5)**, 683-700 (2025).
[17] Minh, D.L., Farnum, N.R. Using bilinear transformations to induce probability distributions. *Communications in Statistics?Theory and Methods* **32(1)**, 1-9 (2003).
[18] Arnold, B.C., SenGupta, A. Probability distributions and statistical inference for axial data. *Environmental and Ecological Statistics* **13** , 271-285 (2006).
[19] Ahn, B.J., Kim, H.M. A new family of semi-circular models: The semi-circular Laplace distributions. *Communications of the Korean Statistical Society* **15(5)**, 775-781 (2008).
[20] Yedlapalli, P., Girija, S.V.S., Rao, A.V.D. On construction of stereographic semicircular models. *Journal of Applied Probability and Statistics* **8(1)**, 75-90 (2013).
[21] Yedlapalli, P., Radhika, A.J.V., Girija, S.V.S., Rao, A.V.D. On trigonometric moments of the stereographic semi-circular gamma distribution. *European Journal of Pure and Applied Mathematics* **10(5)**, 1124-1134 (2017).
[22] Abuzaid, A.H. A half circular distribution for modeling the posterior corneal curvature. *Communications in Statistics?Theory and Methods* **47(13)**, 3118-3124 (2018).
[23] Yedlapalli, P., Sastry, K., Rao, A. On stereographic semi-circular Quasi Lindley distribution. *Journal of New Results in Science* **8(1)**, 6-13 (2019).
[24] Yedlapalli, P., Girija, S.V.S., Rao, A.V.D., Sastry, K.L.N. A half circular distribution for modeling the posterior corneal curvature. *Thai Journal of Mathematics* **18(2)**, 775-781 (2022).
[25] Iftikhar, A., Ali, A., Hanif, M. Half circular modified Burr-III distribution, application with different estimation methods. *PLoS ONE* **17(5)**, e0261901 (2022).
[26] Mohammed, H.J., Mohammed, S.F. On stereographic semi-circular Shankar distribution: Properties and applications. *International Journal of Engineering and Information Systems* **7(9)**, 53-60 (2023).
[27] Awad, N.T., Mohammed, S.F. On stereographic semi-circular three parameter Lindley distribution. *International Journal of Engineering and Information Systems* **8(1)**, 84-91 (2024).
[28] Radhika, A.J.V., Yedlapalli, P., Raju, C.P., Kishore, G.N.V., Sri Krishna, A., Pradeep Kumar, R.L.N. On stereographic semi-circular Erlang distribution with application. *Proceedings on Engineering Sciences* **6(3)**, 1299-1308 (2024).
[29] Semary, H.E., Alshad, K.B., Bengalath, J., Alghamdi, S.M. Semicircular Maxwell-Boltzmann distribution: Application to posterior corneal curvature data. *Journal of Radiation Research and Applied Sciences* **18(2)**, 101471 (2025).
[30] Shanker, R., Sharma, S., Shanker, U., Shanker, R. Janardan distribution and its application to waiting times data. *Indian Journal of Applied Research* **3(8)**, 500-502 (2013).
[31] Lindley, D.V. Fiducial distributions and Bayes' theorem. *Journal of the Royal Statistical Society, Series B* **20**, 102-107 (1958).

© 2026 NSP
Natural Sciences Publishing Cor.